A CASE STUDY REGARDING THE IN-CYLINDER AIR MOTION CHARACTERISTICS IN A MOTORED GASOLINE ENGINE: CFD VS. PIV

George Trică[a], Iorga-Simăn Victor[a], Adrian Clenci[a,b], Stéphane Guilain[c]
Amélie Danlos[b], Rodica Niculescu[a]

[a]University of Pitești, Dept. Automobiles and Transport, 1, Tg. din Vale street, Pitești, Roumanie
[b]Cnam Paris, 292, rue St. Martin, Paris, France
[c]Renault France

*Corresponding author: trica.george@gmail.com

Abstract. Fuel economy is a prime objective in order to meet regulatory and customer demands. Given this context, engine manufacturers are forced to introduce complex systems such as variable valve actuation (VVA). One of the simplest form of a VVA system is what is usually called as variable valve timing (VVT). What's important in these particular cases is in what way the internal aerodynamics and gas exchange phenomena interacts. To study internal aerodynamics, 2 methods are used: an experimental one, employing PIV (particle image velocimetry) technique (for instance) and a numerical one, employing 3D CFD simulation.
In the present study, the internal aerodynamics of a motored VVT gasoline engine is examined by using the 2 methods presented above. The purpose is to see the correlation degree between the experimental results obtained on a transparent single cylinder engine through PIV technique and the ones obtained from a three dimensional CFD (computational fluid dynamics) simulation through RANS (Reynolds-Averaged Navier Stokes) approach. The paper describes the methodology used to perform the CFD simulation, the experimentation and the PIV - CFD comparison; it also discusses about the limitation of the CFD simulation and about the difficulties of such a study.
Keywords: internal aerodynamics, tumble, CFD, PIV.

1. INTRODUCTION

The worldwide concern about the environmental impact of energy conversion systems is the cause of the imposition of strict government regulations relevant to pollutant emissions and fuel-efficiency standards of vehicles. Nowadays, one of the preferred route towards the reduction of both engine exhaust noxious emissions and fuel consumption remains the control of the mixture formation and combustion processes taking place within the engine's cylinders. This is a very complicated task, affected by many variables, amongst which we mention only the ones that affects the engine's internal aerodynamics: design of the manifolds, combustion chamber shape, piston, stroke value.

To investigate an engine's internal aerodynamics, experimental and numerical approaches can be used. An overview of the types of measurements employed in this field is given in [1], [2]. Thus, measurements of the velocity field in steady flow test rigs or transparent engine test benches, using single-point systems, such as hot-wire anemometry or laser Doppler velocimetry (LDV) and/or full field endoscopic imaging for particle image velocimetry (PIV) are quite often employed. Generally, these techniques are able to provide high quality results (even the spatial structure and the temporal resolution of the velocity field [3]) but require good optical access (quartz piston window and cylinder ring) for large fields of view, high speed photography, innovative data analysis methods, and state-of-the-art equipment, which makes them quite expensive. Performing flow measurements in an engine can therefore be difficult because of the complexity of the equipment involved. The high cost and time needed to achieve optimization through bench testing alone has drawn interest of engine developers towards the use of Computational Fluid Dynamics (CFD), codes relying on RANS (Reynolds-Averaged Navier Stokes) analyses. The advantages of numerical investigations are: exactly

prediction of the fluid properties using limited space and time, easier modifications in the existing geometry shapes, representations of fluid characteristics in an interactive way, level of detail unlimited, no expensive to use. According to [4], a challenge to CFD simulation is sometimes the limited availability of suitable experimental data to guide the development and assess the accuracy of the methodology.

This particular study is part of a larger research program [5], which concerns the improvement of the gasoline engine's operation by improving the internal aerodynamics. Experimental and numerical approaches are equally employed. For the experimental part, PIV technique is used on a single cylinder transparent motored engine, as presented in papers [6, 7].

In the present study, the results of 3D CFD simulation featuring RANS approach [8] and PIV experimentation [6, 7] are compared in order to see the degree of correlation. The internal aerodynamics (i.e. in-cylinder air motion characteristics) of the engine submitted to test are analyzed for one particular case.

2. EXPERIMENTATION

2.1. Engine test bench

The experimental setup consists of a single-cylinder transparent engine, coupled to a DC (direct current) electrical driving motor, mounted on a rigid frame isolated by four legs that absorb vibrations. The purpose is to study the in-cylinder air motion characteristics in a motored gasoline engine (i.e. without combustion).

The entire experimental setup is illustrated in figure 1, [6, 7]. It includes: 1 - transparent cylinder, 2 - cylinder head, 3 - exhaust manifold, 4 - inlet splitter, 5 - distribution box, 6 - timing belt, 7 - DC motor.

Fig. 1. Cylinder engine test bench adapted for PIV [6, 7]

The main parameters of the motored transparent engine are presented in Table 1.

Table 1. *Engine main parameters*

Parameter	Value
Bore [mm]	72.0
Stroke [mm]	73.1
Connecting rod length [mm]	128
Piston offset [mm]	0
Cylinder head gasket thickness [mm]	0.7
Compression ratio [-]	12.3
Engine speed [rpm]	1200
Exhaust Valve Opening, EVO [ºCA BBDC]	40
Exhaust Valve Closing, EVC [ºCA ATDC]	6
Intake Valve Opening, IVO [ºCA BTDC]	1
Intake Valve Closing, IVC [ºCA ATDC]	35
NB. Valve timing is given for a 0.2 mm reference lift	

A graphical representation of the exhaust & intake valve lift law is given in figure 2.

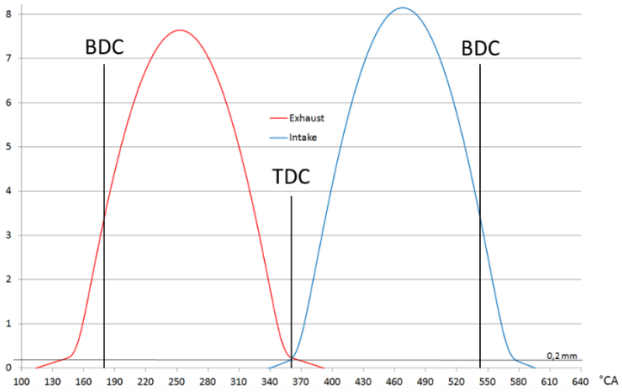

Fig. 2. Valve laws

The experimental apparatus for this particular study consisted of the transparent single-cylinder engine, instrumented to enable accurate acquisition of the instantaneous in-cylinder, intake and exhaust pressure evolutions (figure 3) and instantaneous in-cylinder air velocities through PIV technique (figure 4).

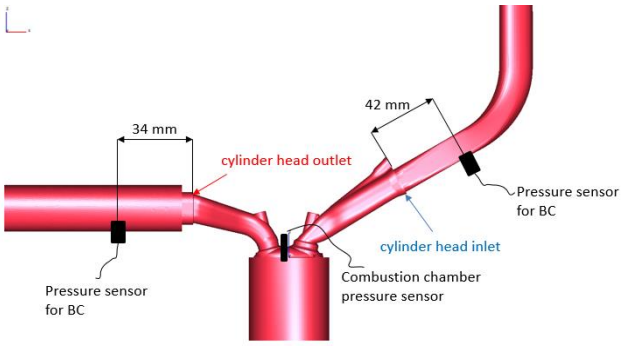

Fig. 3. Sensor positions for pressure acquisitions

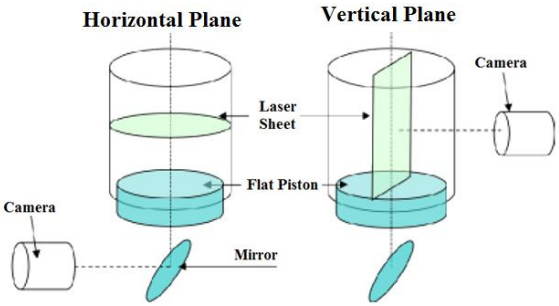

Fig. 4. Horizontal and vertical measuring planes, [7]

For the PIV technique, generally, the flow is inoculated with fine particles part, which is illuminated by a light source. The particles diffuse the light that is recorded on a digital support by passing through an optical system. The acquired image is then analysed by digital processing to obtain the displacement of the particles.

The principle of the velocity measurement is based on two consecutive illuminations of a flow area, separated by a known time interval Δt. The operation is repeated a limited number of times and the set of images pairs obtained can be processed to obtain the velocity field. For this, each image is divided into elementary interrogation cells. The cross-correlation between two corresponding cells in each image is calculated to identify the pattern particles offset. The most likely displacement of the particles in the cell is then given by the position of the correlation peak. Accordingly, by reducing this displacement to the time interval between light flashes was obtained the most probable speed in the interrogation cell.

To obtain quantification for flow interpretation, a large number of plans are necessary. Therefore, measuring planes in horizontal and vertical positions have been made, figure 4.

3. CFD SIMULATION

The main goal of this paper is the analysis of the correlation degree between results concerning the internal aerodynamics obtained via 3D CFD and PIV technique. The CFD simulation was performed with AVL Fire software and it aims to provide quantitative information about the engine's internal aerodynamics for an entire engine cycle. The CFD simulation is of RANS type and was detailed in paper [8].

3.1. Engine geometry modelling

The 3D geometrical shapes of the engine were built using CATIA software. In order to obtain the geometric model needed for the numerical simulation, taking into account the positions of the intake and exhaust pressure sensors (see figure 3), from the initial geometry, we renounced to the outer parts of the intake and exhaust manifolds.

Thus, as seen from figure 5, only the following elements were kept: parts of the intake and exhaust manifolds; intake and exhaust ducts within cylinder head, intake and exhaust valves, combustion chamber, cylinder and piston.

3.2. Boundary and initial conditions

The pressure signals to be used as boundary conditions (BC) at the computational domain inlet and outlet are obtained from experimental measurements performed in the intake and exhaust ducts at a known distance from the cylinder head (Fig. 3). According to figure 6, the pressure inlet BC was applied at 42 mm from the cylinder head inlet and a pressure outlet BC was imposed at 34 mm from surface of the exhaust cylinder head outlet. Also, we apply a BC of mass flow type for the first piston ring to take into consideration the blow-by effect, which in the case of the transparent engine used in the experimentation is more intense due to the special graphite type of ring used to avoid scratching of the engine's transparent cylinder.

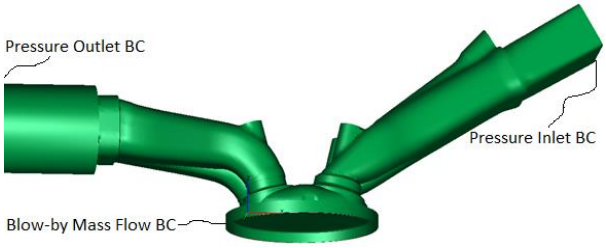

Fig. 5. Engine geometry and boundary conditions

The values used for the above mentioned BCs are presented in details in paper [8]. Walls geometry is considered as impenetrable with an initial temperature at 20°C. In the simulation, air is assumed to be an ideal gas. According to data taken at engine test bench, when exhaust valve begins to open, initial pressure inside the cylinder have been set up at 0.806 bar, 1.029 bar for intake manifold and 1.012 bar for exhaust manifold.

3.3. The mesh and turbulence model

The discretization of the engine computational domain is made through the pre-processing software included in the AVL Fire™, namely the Fame Engine Plus module (FEP). In order to maintain the computational time within reasonable limits, various grid zones are considered active

only in physical domains of interest. When the intake and exhaust valves are closed, the grid is built only in the cylinder, while the intake and exhaust ducts are added at the crank angles for which these volumes are actually put into contact with the cylinder by the valves opening. The cells refinement level, in valve gap area and combustion chamber, has been increased during the period when valves begin to open and close, or the piston is at TDC.

For this mesh, unstructured and structured meshes were used. The unstructured mesh is only necessary for the opening and closing of the valves because the grid has to be re-meshed to avoid degenerated grid cells. The cell shape is hexahedral (for the volumes where structured mesh type was used) and tetrahedral (for the volumes where specific, complicated, geometry was used).

As the mesh is a moving and deformable one, the number of volume type elements varies: 3,179,669 when the piston is at TDC and 2,500,000 when it is at BDC with a minimum 1,277,854 cells for a less-interest zone. Generally, the mesh is a trade-off resulted from the need to obtain good results in reasonable simulation time. For instance, the simulation time of our particular situation (one complete non-combustion engine cycle) was of about 5 days on an Intel Xeon machine (2.66 GHz six core processor and 24 GB of RAM). Generally, when it comes to choosing the right mesh, the independence of the numerical solution with respect to the mesh should be proven.

The chosen turbulence model is the $\kappa - \zeta - f$ recently developed by Hanjalic, Popovac and Hadziabdic [9]. It is a robust modification of the elliptic relaxation model. The aim is to improve numerical stability of the original $\overline{v^2} - f$ model by proposing an eddy viscosity model, which solves a transport equation for the normalized wall-normal velocity scale $\zeta = \overline{v^2}/k$ instead of $\overline{v^2}$. This turbulence variable (ζ) can be regarded as the ratio of the two time scales: scalar k/ε (isotropic), and lateral $\overline{v^2}/k$ (anisotropic). It also introduces a more robust wall boundary condition for f equation, this time f_{wall} is proportional to $1/y^2$ (y is a dimensionless wall distance) instead of $1/y^4$ in the original $\overline{v^2} - f$ model.

Since there are numerous turbulence modelling approaches (e.g. $k - \omega$ model with its two declinations: k – ω standard and *k – ω Shear Stress Transport*; $k - \varepsilon$ model with its three declinations: *$k - \varepsilon$ standard*, *realizable* $k - \varepsilon$ and *$k - \varepsilon$ Re-Normalized Group*), in order to sustain the one chosen, several CFD simulations should be carried out to see which the best is.

Up to now, our CFD simulation was performed only with the $\kappa - \zeta - f$ turbulence model. Other simulations using other turbulence models are currently in progress.

3.4. CFD results

The analysis of the correlation degree between results concerning the internal aerodynamics obtained via 3D CFD using $\kappa - \zeta - f$ turbulence model and PIV technique was performed only after seeing that there is a good agreement between the in-cylinder pressure evolution in the experimentation and in the CFD simulation. As seen from figure 6, the trend predicted by the CFD model is very close to the experimental results, although there are some minor differences, which can be observed on the expansion stroke. These differences may be attributed to the blow-by effect which was not measured but predicted by 1D simulation. Anyway, in the first two strokes the concordance is almost complete. Coming back to the mesh, this agreement presented in figure 6 was the reason for not refining it anymore.

Therefore, as mentioned before, the next step was to start analysing the correlation degree between CFD-RANS and PIV results concerning the in-cylinder air motion characteristics.

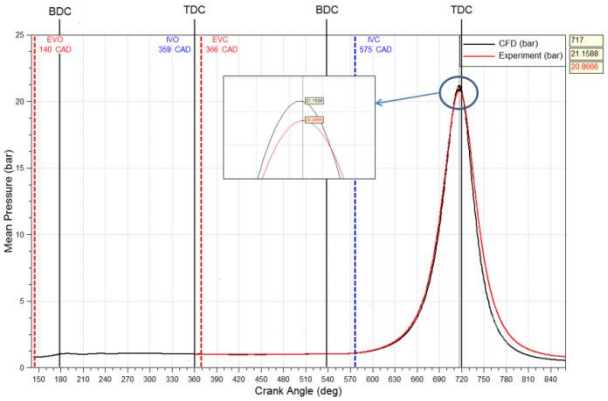

Fig. 6. In cylinder pressure evolution. Experiment – CFD correlation

4. PIV vs. CFD

As mentioned in [6 and 7], the goal of the PIV experimentation was to see the cycle-to-cycle variation of the in-cylinder flow characteristics for a motored engine. As a consequence, 500 engine cycles were acquired. The thorough analysis

presented in [6 and 7] showed that even though the engine was motored at constant speed, in other words, even though it was only about non-combustion cycles, an important cyclic dispersion regarding the internal aerodynamics of the engine occurred. Similar results were also reported in [3].

Since the results obtained with the CFD-RANS approach are for an average engine cycle, then, one question might appear: to which of the 500 cycles acquired with PIV technique this singular CFD cycle should be compared? Certainly, RANS being an averaged approach, then, when it comes to perform a comparative analysis between CFD-RANS results and the ones obtained by using this particular PIV approach, one should compare RANS results with the averaged results of PIV test over the 500 engine cycles.

These being said, the methodology used to perform this comparative analysis (CFD-RANS vs. PIV) is presented subsequently.

As explained in figure 4, the in-cylinder velocities field were created in horizontal and vertical planes. For instance, if tumble motion is at issue, then the analysis should be performed in a vertical plane with piston either in BDC position at the end of the intake stroke or in TDC position at the end of the compression stroke.

Our comparative analysis was focused on the in-cylinder air motion characteristics at the end of the intake stroke. For this particular position, the following grid was used in the vertical plane to recreate the velocity field inside the cylinder when using PIV technique: 62 dots on X axis, respectively 65 dots on Y axis (figure 7, a).

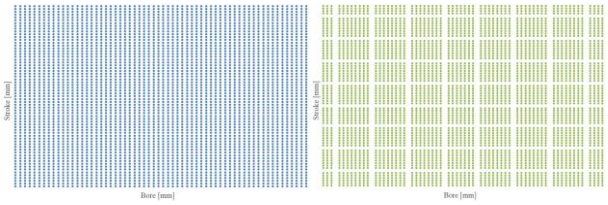

a. PIV *b. common grid: PIV&CFD*

Fig. 7. Grid on the vertical plane

Obviously, the CFD results were obtained on some other grid. In order to be able to perform the comparative analysis we are interested in, one common grid was created (figure 7, b).

Thus, the results concerning the in-cylinder velocities using this common grid are shown in figures 8 and 9. Both figures represent the internal aerodynamics obtained at the end of the intake stroke. Concerning the velocity field obtained from PIV data, figure 9 presents an average situation over the 500 engine cycles acquired.

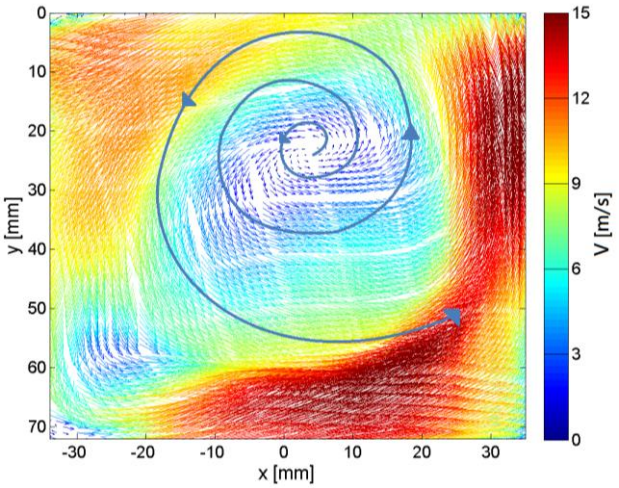

Fig. 8. Velocity field via CFD-RANS

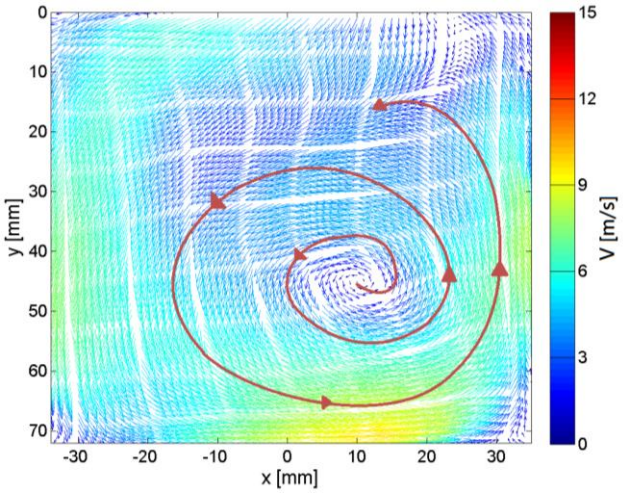

Fig. 9. Velocity field via PIV – averaged over 500 cycles

When analysing the degree of correlation between the results presented in figures 8 and 9, one can see that the only similarity can be found in the rotational sense of the tumble motion. Concerning the center of this tumble motion, the averaged PIV results show that it is displaced downward and to the right part of the cylinder with respect to the CFD-RANS results. The magnitude of the flow velocities is also different (a maximum of 15 m/s for the CFD-RANS results and a maximum of 9 m/s for the averaged PIV results). However, the maximum values of the velocities in both cases are (as expected) in the peripheral area of the tumble vortex. One cause of this disagreement may come from imposing pressure type BCs too close to the cylinder. In other words, in the real situation, the intake runner bent pipe

coming from above the point where BCs were imposed is expected to induce a secondary motion leading to inhomogeneous velocity profile across the intake port entrance which is not taken into account in the current simulation.

Taking into account the cycle-to-cycle variations mentioned before and the weak agreement between the data presented in figures 8 and 9, at this stage, the next step was to find the best PIV cycle which is close enough to the CFD simulation. Thus, two methods were used:

1. tumble ratio comparative analysis
2. calculation the difference between the instantaneous velocity on X and Y directions for each grid point and then counting the grid points for which the difference is under an arbitrary threshold of 1 m/s

The tumble ratio was found with the following relation:

$$T_r = \frac{\omega_{FK}}{\omega_{Mot}}, \qquad (1)$$

where:

- $\omega_{FK} = \frac{\sum \omega_i r_i^2}{\sum r_i^2}$ – angular velocity corresponding to the velocity distribution;
- $\omega_i = \frac{W_i}{r_i}$ – local angular velocity;
- $\omega_{Mot} = \frac{\pi n_{mot}}{30}$ – angular velocity of the engine.

Figure 10 shows the results of the tumble ratio comparative analysis. As seen, cycle number 103 from the PIV experimentation has the closest value to the CFD result ($T_{r\ PIV\#103} = 1.56$ vs. $T_{r\ CFD} = 2.08$).

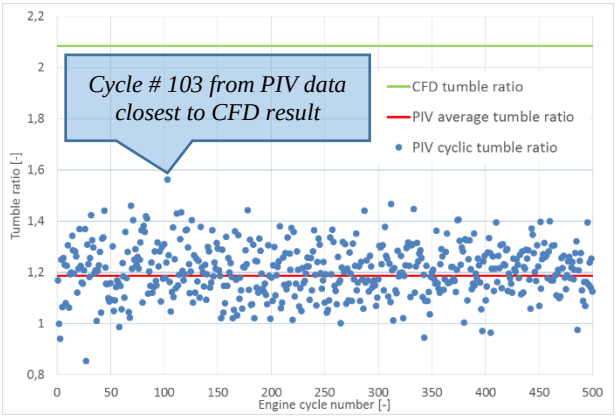

Fig. 10. Tumble ratio comparative analysis

Figure 11 shows the results of applying the second method: the closest PIV cycle to the CFD simulation is the 14th one.

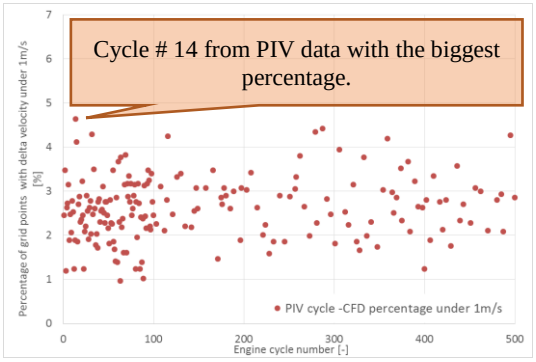

Fig. 11. Percentage of grid points with differences between the instantaneous velocity on X and Y directions lower than 1m/s

This 14th cycle has the highest percentage of points (4.64%) from the common grid with differences between the instantaneous velocity on X and Y directions lower than 1m/s. Actually, the result is not at all satisfying.

The flow velocity fields for the 103rd and 14th PIV cycles are presented in figures 12 and 13.

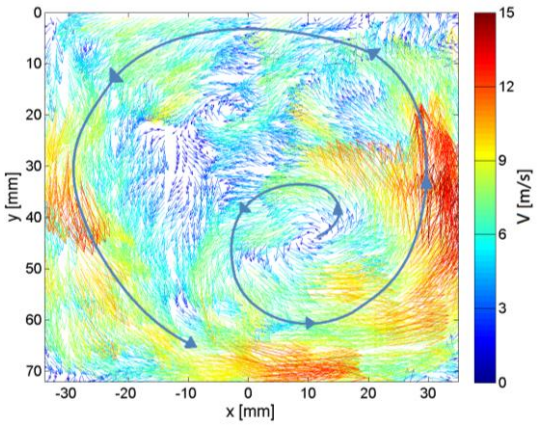

Fig. 12. Flow velocity field, PIV cycle #103

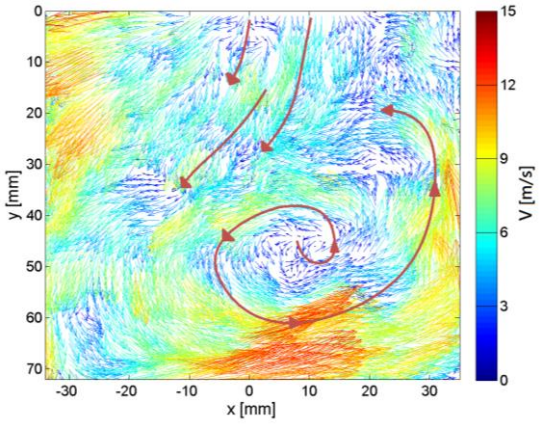

Fig. 13. Flow velocity field, PIV cycle #14

Now, when performing a comparison between the results presented in figures 12 and 13 with the ones from figure 8, one can see there is a much more resemblance between the CFD cycle and the 103rd PIV cycle. The velocities in the peripheral

area are much closer to the ones obtained through CFD simulation.

Concerning the PIV cycle number 14, the tumble vortex suffers a distortion, meaning that it seems not to be as organized as before. This makes it a more different cycle with respect to the CFD cycle.

5. CONCLUSIONS AND FUTURE WORKS

The paper dealt with a case study on the attempt to find a correlation between CFD data obtained through RANS approach and experimental data obtained through PIV technique.

The findings of this study can be summarized as follows:

- the expectation to have a good agreement between RANS results and the ones obtained by averaging the PIV data over the 500 engine cycles was not met;
- some causes of this disagreement were identified (e.g. imposing pressure type BCs too close to the cylinder) but need to be checked by future studies;
- however, taking into consideration the cycle-to-cycle variation recorded while performing the PIV experimentation, some resemblances may be found between CFD-RANS results and the ones from PIV by using one of the two methods presented in this paper; however, this kind of comparison might not be that relevant.

Thus, future analyses will seek the means to obtain an acceptable concordance between the averaged PIV cycle over the 500 cycles and the RANS cycle by exploring either different BCs (e.g. instead of pressure type, mass flow type) or different position for pressure type BCs. Equally, the influence of the turbulence models upon the RANS results concerning the in-cylinder air motion characteristics is to be explored. Once the agreement between the averaged PIV cycle and RANS cycle will be found, the next step will be to see the effect of the implementation of Large Eddy Simulation (LES) technique which seems to be more suited when it comes to simulate, understand and control the cycle-to-cycle variations of the internal aerodynamics of an IC engine.

ACKNOWLEDGMENTS

The authors would like to express their gratitude to Dr. Wolfgang Schwarz from AVL France for supporting the study.

REFERENCES

[1] P. V Farrell, *"Examples of in-cylinder velocity measurements for internal combustion engines"*, Proc. Inst. Mech. Eng. Part D J. Automob. Eng., vol. 221, pp. 675–697, 2007.

[2] D. Ramajo, A. Zanotti, and N. Nigro, *"In-cylinder flow control in a four-valve spark ignition engine: numerical and experimental steady rig tests,"* Proc. Inst. Mech. Eng. Part D-Journal Automob. Eng., vol. 225, no. D6, pp. 813–828, 2011.

[3] D. Liu, T. Wang, M. Jia, and G. Wang, *"Cycle-to-cycle variation analysis of in-cylinder flow in a gasoline engine with variable valve lift"*, Exp. Fluids, vol. 53, no. 3, pp. 585–602, 2012.

[4] A. C. Clenci, V. Iorga-Simăn, M. Deligant, P. Podevin, G. Descombes, and R. Niculescu, *"A CFD (computational fluid dynamics) study on the effects of operating an engine with low intake valve lift at idle corresponding speed"*, Energy, vol. 71, pp. 202–217, 2014.

[5] *"Calculation of unsteady in-cylinder flow of Gasoline engines with FIRE software"* Scientific Cooperation between University of Pitești, Renault, AVL, 2015-2017.

[6] Cao Y, Kaiser E, Borée J, Noack BR, Thomas L, Guilain S - *"Cluster-based analysis of cycle-to-cycle variations: application to internal combustion engines"*, Exp. Fluids 2014; 55: 1837-1845

[7] Cao Y – "*Sensibilité d'un écoulement de rouleau compressé et des variations cycle à cycle associées à des paramètres de remplissage moteur*", Thèse de doctorat, Ecole Nationale Supérieure de mécanique et d'aérotechnique 2014.

[8] G. Trică, V. Iorga-Simăn, A. Clenci, R. Niculescu, A. Trică – *"A CFD approach for the study of the in-cylinder air motion characteristics in a motored gasoline engine"*, Revista Inginerilor de Automobile, serie nouă, nr. 38 (martie) / 2016, pg. 12, ISSN 1842 – 4074

[9] Hanjalic, Popovac, and Hadziabdic, *"About the $\kappa - \zeta - f$ turbulence model"* AVL Fire Documentation, 2004.